Stabilization of Sets Parametrized by a Single Variable: Application to Ship Maneuvering

Roger Skjetne* **Andrew R. Teel**† **Petar V. Kokotović**†

Abstract

We consider the problem of stabilizing sets parametrized by a single variable. Our approach is based on the solution to the maneuvering problem. In this problem, the state of the system is driven to a path that coincides with the set, and the particular location on the path is determined dynamically from the value of the state. Within this control structure, we induce a separation of time scales between the task of selecting the point on the path closest to the state, and the task of driving the state towards the path. In addition to uniform global convergence to the path, which is achieved without a separation of time scales, the separation of time scales allows us to achieve *near forward invariance* of the path from a large range of initial conditions. This idea is first illustrated on a simple double integrator with the path corresponding to the unit circle, and then it is discussed for systems in strict feedback form. Finally, the theory is applied to the problem of maneuvering a ship into a harbour.

Keywords: Nonlinear control; Maneuvering; Trajectory tracking; Set stabilization; Gradient minimization; Ship control.

1 Introduction

In many practical control applications (vehicles, robot manipulators), the task is to force the output or state of the dynamical plant to converge to and follow a path or curve that is not necessarily parametrized by time. Extending the work in [1, 2], the control objective for *The Maneuvering Problem* in [3, 4] involves two tasks. The first, called the *Geometric Task*, is to force the state x to converge to and stay on a desired path ξ that is continuously parametrized by a scalar variable θ. The second task, called the *Dynamic Task*, is to make the variable θ satisfy a desired dynamic behavior along the path, usually as a speed assignment for $\dot{\theta}$. This problem formulation can also be viewed as a *set stabilization problem* where the desired path $\xi(\theta)$ is represented by a target set Ξ. The geometric task then corresponds to rendering Ξ uniformly attractive, whereas the dynamic task corresponds to satisfying a desired dynamic behavior within the set.

In this paper we draw on ideas from the maneuvering design in [4], and apply those to set stabilization problems. The target set Ξ is made *uniformly globally attractive* through the asymptotic stabilization of a subset Ξ_θ. However, Ξ is not, in general, made *forward invariant*, and thus not

*R. Skjetne is with the Department of Engineering Cybernetics, Norwegian University of Science and Technology (NTNU), Trondheim, Norway. E-mail: skjetne@ieee.org

†A. R. Teel and P. V. Kokotović are with the Center of Control Engineering and Computation, University of California, Santa Barbara, USA. E-mails: teel@ece.ucsb.edu and petar@ece.ucsb.edu

uniformly globally asymptotically stable. To this end, we instead equip the controller dynamics with a gradient optimization algorithm that possesses a tuning parameter which can be adjusted to make Ξ "nearly" forward invariant. This property is called *"near forward invariance"* of Ξ, and together with uniform global attractivity it renders Ξ *"nearly stable"*.

To achieve the desired result, a separation of time scales is induced between the gradient algorithm that selects the path parameter θ to minimize the weighted distance between x and $\xi(\theta)$, and the stabilization algorithm that drives x to $\xi(\theta)$. The uniform global attractivity of Ξ follows from the analysis in [4] while the near uniform asymptotic stability of Ξ follows from singular perturbation analysis, and in particular the results in [5].

Notations: Abbreviations like GS, LAS, LES, UGAS, UGES, etc., are G for Global, L for Local, S for Stable, U for Uniform, A for Asymptotic, and E for Exponential. A superscript denotes partial differentiation: $f^{x}(x,y) := \frac{\partial f}{\partial x}$, $f^{y}(x,y) := \frac{\partial f}{\partial y}$, $f^{x^2}(x,y) := \frac{\partial^2 f}{\partial x^2}$. The Euclidian vector norm is $|x| := \sqrt{x^\top x}$, and the distance to the set $\mathcal{A}$ is $|x|_{\mathcal{A}} := \inf_{a\in\mathcal{A}} |x-a|$. For a matrix $P = P^\top > 0$, let $p_m := \lambda_{\min}(P)$ and $p_M := \lambda_{\max}(P)$.

1.1 The double integrator and stabilization of the unit circle

We consider the double integrator

$$\begin{aligned} \dot{x}_1 &= x_2 \\ \dot{x}_2 &= u \end{aligned} \tag{1.1}$$

and the task of stabilizing the set

$$\mathcal{A} := \left\{ x \in \mathbb{R}^2 : x^\top x = 1 \right\} \tag{1.2}$$

without creating any equilibria in $\mathcal{A}$. By converse Lyapunov theory (see, for example, [6]), there does not exist a continuous or discontinuous time-invariant state feedback control that renders the unit circle GAS. (In the case of discontinuous feedback, this statement applies when the solution concept used is that due to Filippov, for example; see [7].) The reasoning is this: If such a feedback existed there would exist a smooth Lyapunov function demonstrating GAS of the circle. In particular, this function would be positive definite with respect to the circle and would have a directional derivative, in the direction of the closed-loop vector field, that is negative definite with respect to the circle. The Lyapunov function would obtain its minimum on the circle, and it would therefore have a maximum inside the circle. At the maximum, its gradient would be zero and so the directional derivative in the direction of the closed-loop could not be negative. So there must not be a Lyapunov function, which implies that GAS cannot be achieved by such a control.

An alternative is to try to stabilize the set

$$\mathcal{A}_\theta := \left\{ (x,\theta) : x = \begin{bmatrix} \cos\theta \\ -\sin\theta \end{bmatrix} \right\} \tag{1.3}$$

for the system (1.1) and

$$\dot{\theta} = 1. \tag{1.4}$$

A control rendering the set $\mathcal{A}_\theta$ GAS will steer (x,θ) to the set $\mathcal{A}\times\mathbb{R}$ since

$$\begin{bmatrix} \cos\theta \\ -\sin\theta \end{bmatrix}^\top \begin{bmatrix} \cos\theta \\ -\sin\theta \end{bmatrix} = 1$$

and thus $\mathcal{A}_\theta \subseteq \mathcal{A} \times \mathbb{R}$. However, choosing to stabilize $\mathcal{A}_\theta$ under the constraint (1.4) may introduce large transients in the distance to $\mathcal{A}\times\mathbb{R}$. In an attempt to control these transients, we will consider controlling θ as well. Therefore, we consider the control

$$\begin{aligned} \dot{\theta} &= 1 + \mu\omega\left(x_1, x_2, \theta\right), \qquad \mu > 0 \\ u &= \alpha\left(x_1, x_2, \theta\right) \end{aligned} \tag{1.5}$$

for the system (1.1), and we show that it renders the set $\mathcal{A}_\theta$ UGES and achieves good performance for large μ. To design the functions ω and α in (1.5) we select a Hurwitz matrix

$$A := \begin{bmatrix} 0 & 1 \\ -k_1 & -k_2 \end{bmatrix}$$

and let $P = P^\top > 0$ be such that $A^\top P + PA = -Q$ where $Q = Q^\top > 0$. Using

$$V\left(x, \theta\right) := \left(x - \xi(\theta)\right)^\top P \left(x - \xi(\theta)\right) \tag{1.6}$$

$$\xi\left(\theta\right) = \begin{bmatrix} \xi_1(\theta) \\ \xi_2(\theta) \end{bmatrix} := \begin{bmatrix} \cos\theta \\ -\sin\theta \end{bmatrix} \tag{1.7}$$

and $K := [k_1\ k_2]$, we assign ω and α in (1.5) as

$$\omega\left(x, \theta\right) = -V^\theta\left(x, \theta\right) = 2\left(x - \xi(\theta)\right)^\top P\xi^\theta(\theta) \tag{1.8}$$

$$\alpha\left(x, \theta\right) = -K\left(x - \xi(\theta)\right) + \xi_2^\theta(\theta). \tag{1.9}$$

Differentiating (1.6) along the solutions of the resulting closed-loop equations

$$\begin{aligned} \dot{x} &= A\left(x - \xi(\theta)\right) + \xi^\theta(\theta) \\ \dot{\theta} &= 1 - \mu V^\theta(x, \theta) \end{aligned} \tag{1.10}$$

gives

$$\begin{aligned} \dot{V}(x, \theta) &= -\left(x - \xi(\theta)\right) Q \left(x - \xi(\theta)\right) - \mu V^\theta(x, \theta)^2 \\ &\leq -q_m \left|x - \xi(\theta)\right|^2 \leq -cV(x, \theta) \end{aligned}$$

where $c := \frac{q_m}{p_M}$. It follows that $|x(t) - \xi(\theta(t))| \leq \sqrt{\frac{p_M}{p_m}} e^{-\frac{c}{2}t} \left|x(0) - \xi(\theta(0))\right|$ holds, and the set $\mathcal{A}_\theta$ is therefore UGES. By definition, $|x|_\mathcal{A} = \inf_\theta |x - \xi(\theta)|$. We let $\bar{\theta}(x)$ satisfy $|x|_\mathcal{A} = \left|x - \xi(\bar{\theta})\right|$. Then, since $|x(t)|_\mathcal{A} \leq |x(t) - \xi(\theta(t))| \leq |x(t)|_\mathcal{A} + 2$, we also have

$$|x(t)|_\mathcal{A} \leq \sqrt{\frac{p_M}{p_m}} e^{-\frac{c}{2}t} \left[|x(0)|_\mathcal{A} + 2\right], \qquad \forall t \geq 0 \tag{1.11}$$

which establishes uniform global attractivity of the set $\mathcal{A}\times\mathbb{R}$. This is a prerequisite for the objective we consider in this problem. Stability of $\mathcal{A}$, however, has not been achieved since this set is not forward invariant.

To instead obtain the aforementioned *"near forward invariance"* property, we induce a two time-scale behavior of the closed-loop system (1.10) by increasing μ. Letting $\varepsilon = \frac{1}{\mu}$ be small, allows us to analyze (1.10) as a singularly perturbed system (see [5, 8, 9]). Let the fast time scale be $t_f = \frac{1}{\varepsilon}t$ and define $x' := \frac{dx}{dt_f}$. Then the closed-loop can be written as

$$x' = \varepsilon A\left(x - \xi(\theta)\right) + \varepsilon\xi^\theta(\theta), \qquad \theta' = \varepsilon - V^\theta(x, \theta).$$

The rapid transient of θ is approximately described by the boundary layer system at $\varepsilon = 0$:

$$\theta' = -V^{\theta}(x, \theta) \tag{1.12}$$

where x is fixed since $x' = 0$ for $\varepsilon = 0$. Clearly, (1.12) is a continuous gradient algorithm which minimizes V with respect to θ for any fixed x. For a given x, the level curves of $\xi \mapsto (x - \xi)^{\top} P (x - \xi)$ are shown in Figure 1. The four values of θ satisying $V^{\theta}(x, \theta) = 0$ are given by the locations where

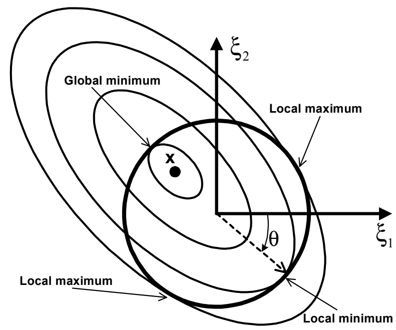

Figure 1: Level sets of $V(x, \cdot)$ for a fixed x, that is, for the function $\xi \mapsto (x - \xi)^{\top} P (x - \xi)$ where the circle, parametrized by θ, is the constraint set for ξ.

the path $\xi(\theta)$, defined in (1.7) and indicated as a solid curve in Figure 1, is tangent to a level set of $\xi \mapsto (x - \xi)^{\top} P (x - \xi)$. These four values of θ correspond to the two local maxima and two local minima of $\theta \mapsto V(x, \theta)$. The global minimum is the value of interest, and it is denoted $\theta_V(x)$. The function $\theta_V(\cdot)$ can be shown to be locally Lipschitz for x near the unit circle. The function $\xi(\theta_V(x))$ is substituted into (1.10) to obtain *the reduced system*

$$\dot{x} = A\left(x - \xi(\theta_V(x))\right) + \xi^{\theta}\left(\theta_V(x)\right) \tag{1.13}$$

which approximately describes the motion of x in time-scale t. This motion is restricted to the slow manifold $\mathcal{M}_{\varepsilon}$ which is ε-close to the manifold $\mathcal{M}_{\theta}$ defined by

$$V^{\theta}(x, \theta_V(x)) = -2\left(x - \xi(\theta_V(x))\right)^{\top} P \xi^{\theta}(\theta_V(x)) = 0. \tag{1.14}$$

This restriction is the result of the gradient optimization which rapidly positions θ to the most favourable position from which x is to converge to the desired circle $x_1^2 + x_2^2 = 1$. This convergence is established by differentiating $W(x) := V(x, \theta_V(x))$ with respect to t along the solutions of the reduced system (1.13). Employing the identity (1.14), this derivative is

$$\dot{W} = -\left[x - \xi(\theta_V(x))\right]^{\top} Q \left[x - \xi(\theta_V(x))\right] \le -q_m \left|x - \xi(\theta_V(x))\right|^2 \le -cW(x(t))$$

which implies

$$\begin{aligned}
|x(t)|_{\mathcal{A}} &= \left|x(t) - \xi(\bar{\theta}(x(t)))\right| \le \left|x(t) - \xi(\theta_V(x(t)))\right| \\
&\le \sqrt{\frac{1}{p_m} W(x(t))} \le \sqrt{\frac{1}{p_m} W(x(0))} e^{-\frac{c}{2}t} \le \sqrt{\frac{1}{p_m} V(x(0), \bar{\theta}(x(0)))} e^{-\frac{c}{2}t} \\
&\le \sqrt{\frac{p_M}{p_m}} \left|x(0) - \xi(\bar{\theta}(x(0)))\right| e^{-\frac{c}{2}t} = \sqrt{\frac{p_M}{p_m}} \left|x(0)\right|_{\mathcal{A}} e^{-\frac{c}{2}t} \qquad (1.15)
\end{aligned}$$

and therefore shows that the set $\mathcal{A}$ is ULES for the **reduced system** (1.13). The standard approximation theorems of singular perturbation analysis guarantee that the solutions of the designed closed-loop system (1.10) are ε-close, on compact time intervals, to the corresponding trajectories composed of the boundary layer transient of $\theta(t)$ and the subsequent motion $x(t)$ of the reduced system with $\theta(t) = \theta_V(x(t))$. With proper initialization, $|x(0)|_{\mathcal{A}}$ sufficiently small and $\theta(0)$ in the region of convergence of $\theta_V(x(0))$, it follows from the results of [5] that for any $\delta > 0$ there exists $\mu^* > 0$ such that $\mu \geq \mu^*$ implies that

$$|x(t)|_{\mathcal{A}} \leq \sqrt{\frac{p_M}{p_m}}\, |x(0)|_{\mathcal{A}}\, e^{-\frac{c}{2}t} + \delta, \qquad \forall t \geq 0 \tag{1.16}$$

holds for (1.10). The behavior of the solution to the true system (1.10) will therefore be δ-close to the behavior, characterized by the bound (1.15), of the reduced system, and this yields the desired near forward invariance property.

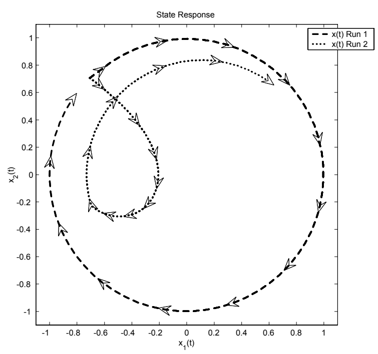

Figure 2: State responses projected into the (x_1, x_2)-plane.

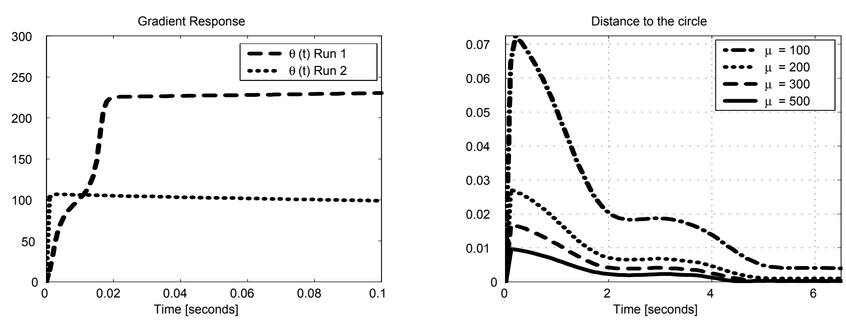

Figure 3: **a)** Time-plots of $\theta(t)$: Rapid transients to the global minimum in Run 1, and a local minimum in Run 2. **b)** Initial error transients of $|x(t)|_{\mathcal{A}}$ for increasing gains μ in the case of a unique minimum.

Figures 2 and 3 show the responses of $x(t)$ and $\theta(t)$ in a simulation, using Matlab$^{\text{TM}}$ and Simulink$^{\text{TM}}$, with $k_1 = 2$, and $k_2 = 1$. Initial positions were $x(0) = [-\frac{\sqrt{2}}{2}\ \frac{\sqrt{2}}{2}]^\top$ (on the circle at the angle $225\,^\circ$) and $\theta(0) = 0\,^\circ$. Figures 2 and 3a) show the responses for $\mu = 500$. In *Run 1,* $V(x(0), \cdot)$ only had one unique initial minimum at $\theta_V(x(0)) = 225\,^\circ$, to which $\theta(t)$ rapidly converges. Thus, the initial transient in the distance to the circle is small, and $x(t)$ stays close for all time (and eventually converges). In *Run 2,* on the other hand, we change the P-matrix so that

$V(x(0),\cdot)$ has an initial local minimum at $\underline{\theta} = 108^\circ$. Since $\theta(0)$ is in the basin of attraction of $\underline{\theta}$, it rapidly converges to $\underline{\theta}$ and causes the bad transient of $x(t)$. In Figure 3b), the responses correspond to the unique minimum case in Run 1 for different gains μ. It is seen that the excursion of $x(\cdot)$ from the circle decreases as μ increases.

2 Review of Maneuvering

In [4] the *Maneuvering Problem* is defined as solving two tasks, referred to as the *Geometric Task* and the *Dynamic Task*. Given a desired *parameterized path* $\xi(\theta)$, the former task is to force the plant state x to converge to the path ξ, and the latter task, stated as a speed assignment along the path, is to force the speed $\dot{\theta}$ to track a desired speed υ_s. Hence, the limit relations

$$\lim_{t\to\infty} [x(t) - \xi(\theta(t))] = 0 \tag{2.17}$$

$$\lim_{t\to\infty} \left[\dot{\theta}(t) - \upsilon_s(\theta(t), t)\right] = 0 \tag{2.18}$$

must hold, where υ_s is a bounded and $\mathcal{C}^{n-1}$ design function. Solving these tasks ensures an overall desired behavior of the plant in the state space, and we call this *maneuvering.*

The design procedure proposed in [4] is applicable to systems in the form

$$\begin{aligned} \dot{x}_1 &= G_1(\bar{x}_1)\, x_2 + f_1(\bar{x}_1) \\ \dot{x}_2 &= G_2(\bar{x}_2)\, x_3 + f_2(\bar{x}_2) \\ &\vdots \\ \dot{x}_n &= G_n(\bar{x}_n)\, u + f_n(\bar{x}_n) \end{aligned} \tag{2.19}$$

$$y = h(x_1) \tag{2.20}$$

where $x_i \in \mathbb{R}^m$, $i = 1, \ldots, n$ are the states and $\bar{x}_i$ denotes the vector $\bar{x}_i = \left[x_1^\top\ x_2^\top\ \ldots\ x_i^\top\right]^\top$, $y \in \mathbb{R}^m$ is the output, and $u \in \mathbb{R}^m$ is the control. The matrices $G_i(\bar{x}_i)$ and $h^{x_1}(x_1)$ are invertible for all $\bar{x}_i$, the output map $h(x_1)$ is a diffeomorphism, and all functions are smooth. Let a uniformly bounded desired path be

$$\mathbf{Y}_d := \{y \in \mathbb{R}^m :\ y = y_d(\theta),\ \theta \in J_\theta \subseteq \mathbb{R}\}. \tag{2.21}$$

To solve the maneuvering problem with respect to (2.21), the design procedure in [4] constructs a global feedback transformation $u = \alpha_n(\bar{x}_n, \theta, t)$ that converts the system (2.19) into the form

$$\dot{z} = A(x,\theta,t)\, z(x,\theta,t) + g(x,\theta,t)\, \omega_s \tag{2.22}$$

where $x = \bar{x}_n$, $\omega_s := \upsilon_s(\theta, t) - \dot{\theta}$, $z := col(z_1, \ldots, z_n)$, $z_1 := y - y_d(\theta)$, $z_i := x_i - \alpha_{i-1}(\bar{x}_{1-1}, \theta, t)$, $i = 2, \ldots, n$, and α_{i-1} are *virtual controls* in the design. For $\upsilon_s(\theta, t) \neq 0$ the tangent vector $g(x,\theta,t) = -z^\theta(x,\theta,t)$ vanishes if and only if the vector $\xi_{cv}(\theta) = col\{y_d^\theta(\theta),\ y_d^{\theta^2}(\theta), \ldots,\ y_d^{\theta^n}\}$ vanishes.

For simplicity, let $\upsilon_s = \upsilon_s(\theta)$ be specified independent of time so that t is eliminated in all the above functions, and the closed-loop (2.22) becomes time-invariant. Based on the output path

$y_d(\theta)$, the design recursively constructs a path $\xi(\theta)$ in the state space which is the explicit solution to $z(x,\theta)=0$, and is represented by the set

$$\Xi_\theta := \{(x,\theta)\in\mathbb{R}^{nm}\times\mathbb{R}:\ z(x,\theta)=0,\ \theta\in J_\theta\}$$
$$= \left\{ (x,\theta): \begin{array}{l} x_1=\xi_1(\theta)=h^{-1}(y_d(\theta)) \\ x_2=\xi_2(\theta)=\alpha_1(\xi_1(\theta),\theta)=G_1^{-1}\left[-f_1+(h^{x_1})^{-1}\,y_d^\theta\upsilon_s\right] \\ x_3=\xi_3(\theta)=\alpha_2(\xi_1(\theta),\xi_2(\theta),\theta)=G_2^{-1}\left[-f_2+\alpha_1^{x_1}\left(G_1\xi_2+f_1\right)+\alpha_1^\theta\upsilon_s\right] \\ \quad\vdots \\ x_n=\xi_n(\theta)=\alpha_{n-1}(\xi_1(\theta),\ldots,\xi_{n-1}(\theta),\theta) \\ \qquad\qquad =G_{n-1}^{-1}\left[-f_{n-1}+\sum\limits_{i=1}^{n-2}\alpha_{n-2}^{x_i}\left(G_i\xi_{i+1}+f_i\right)+\alpha_{n-2}^\theta\upsilon_s\right] \end{array} \right\} \tag{2.23}$$

Along with the recursive design follows a control Lyapunov function (CLF) and its derivative along the solutions of (2.22):

$$V(x,\theta) = z(x,\theta)^\top P z(x,\theta), \qquad P=P^\top>0 \tag{2.24}$$
$$\dot V = -z(x,\theta)^\top Q z(x,\theta) - V^\theta(x,\theta)\omega_s, \qquad Q=Q^\top>0. \tag{2.25}$$

From (2.25) it is seen[1] that any assignment of $\omega_s=\omega_s(x,\theta)$ such that $V^\theta(x,\theta)\omega_s(x,\theta)$ gives

$$\dot V \le -z(x,\theta)^\top Q z(x,\theta) \le -cV(x,\theta), \qquad c:=\frac{q_m}{p_M} \tag{2.26}$$

and thus $z=0$ is UGES for (2.22). This implies that $z_1(t)=y(t)-y_d(\theta(t))\to 0$ as $t\to\infty$ which solves the geometric task. In the original coordinates (x,θ) the closed-loop can be written in the affine form

$$\dot x = z^x(x,\theta)^{-1}[A\,(x,\theta)\,z\,(x,\theta)+g\,(x,\theta)\,\upsilon_s(\theta)] = \tilde f\,(x,\theta)+\tilde g\,(x,\theta)\,\upsilon_s\,(\theta) \tag{2.27}$$
$$\dot\theta = \upsilon_s\,(\theta)-\omega_s(x,\theta) \tag{2.28}$$

where the Jacobian $z^x(x,\theta)$ is lower triangular and always invertible, and $\tilde f$ and $\tilde g$ have the properties that $\tilde f\,(s,\theta)\,|_{s=\xi(\theta)}=0$ and $\tilde g\,(s,\theta)\,|_{s=\xi(\theta)}=\xi^\theta\,(\theta)$. Therefore, on the path, $z=0$, the vector field (2.27) satisfies the flow $\dot x=\xi^\theta\,(\theta)\,\upsilon_s\,(\theta)$ as required by the maneuvering objective. Assuming the derivative $\xi^\theta(\theta)$ is bounded, then there exist class-$\mathcal{K}_\infty$ functions γ_1 and γ_2 that are linear for small arguments, such that

$$\gamma_1(|x-\xi(\theta)|)\le|z(x,\theta)|\le\gamma_2(|x-\xi(\theta)|). \tag{2.29}$$

Since $z\,(t)\to 0$ exponentially, the solution of (2.27) converges to a one-dimensional invariant manifold defined by $z\,(x(t),\theta(t))\equiv 0$. On this manifold, the solution by (2.22) satisfies

$$0=g\,(x,\theta)\,|_{x=\xi(\theta)}\left[\upsilon_s\,(\theta)-\dot\theta\right]$$

and if $g\,(\xi(\theta),\theta)$ is non-vanishing along the path, then $\dot\theta(t)\to\upsilon_s(\theta(t))$ as $t\to\infty$ which solves the dynamic task. Otherwise, if the assignment of ω_s has the property, $z=0\Rightarrow\omega_s=0$, then the dynamic task is clearly solved by (2.28).

[1]Note that V^θ is in [4] referred to as a tuning function $\tau(x,\theta)=-V^\theta(x,\theta)$.

3 Stabilization of sets parametrized by a single variable

In many contexts, stabilization of sets parameterized by a single variable is interesting. Obvious examples are control of robots, vessels, and vehicles where a desired path can be characterized by such a set. In fact, all applications where the states should be forced to a one dimensional manifold or subset in the state space fall into this category.

With the parametrization $\xi(\theta)$ from (2.23), define the target set

$$\Xi := \{x \in \mathbb{R}^{nm} : \ x = \xi(\phi), \ \phi \in J_\theta \subseteq \mathbb{R}\} \tag{3.30}$$

for the system (2.19). As shown in the motivational example in Section 1.1, stabilization of Ξ may involve some difficulties. While uniform global attractivity can be obtained with relative ease, the forward invariance property may be hard to achieve. Therefore, the set Ξ cannot, in general, be rendered GAS. The design procedure in [4], revisited in the last section, achieves global asymptotic convergence to a subset of $\Xi \times J_\theta$ but not stability of $\Xi \times J_\theta$. In what follows we abandon stability in the strict sense and instead construct a control algorithm that ensures *"near stability"*.

3.1 Main result: Rendering the target set "nearly" stable

To achieve near stability of $\Xi \times J_\theta$, the set has to be uniformly globally attractive, and additionally, we need the algorithm to contain a parameter that can be tuned to make the set *"near forward invariant"*. Define the distance functions:

$$\begin{aligned}
|x|_\Xi &:= \inf_\theta |x - \xi(\theta)| = \left|x - \xi(\bar{\theta}(x))\right| \\
|x|_{\Xi,V} &:= \inf_\theta \sqrt{V(x,\theta)} = \sqrt{V(x,\theta_V(x))} \\
|x|_{\Xi,z} &:= \inf_\theta |z(x,\theta)| = |z(x,\theta_z(x))|
\end{aligned}$$

where $\bar{\theta}$, θ_V and θ_z are the corresponding values that satisfy the infimums. Recall that from the triangular inequality $|x - \xi(\theta)| \leq |x|_\Xi + \left|\xi(\bar{\theta}(x)) - \xi(\theta)\right|$. If (2.26) hold, then for all x

$$V(x(t),\theta(t)) \leq V(x(0),\theta(0))e^{-ct}$$

where c is defined in (2.26). Define the class-$\mathcal{KL}$ function β as

$$\beta(s, \ t) := \gamma_1^{-1}\left(\sqrt{\frac{p_M}{p_m}}\gamma_2(s)\, e^{-\frac{c}{2}t}\right) \tag{3.31}$$

and let $d := \left|\xi(\bar{\theta}(x(0))) - \xi(\theta(0))\right|$. This gives the following relationships

$$\begin{aligned}
|x(t)|_\Xi &\leq |x(t) - \xi(\theta_z(x(t)))| \leq \gamma_1^{-1}\left(|x(t)|_{\Xi,z}\right) \leq \gamma_1^{-1}\left(|z(x(t),\theta_V(x(t)))|\right) \\
&\leq \gamma_1^{-1}\left(\sqrt{\frac{1}{p_m}}\,|x(t)|_{\Xi,V}\right) \leq \gamma_1^{-1}\left(\sqrt{\frac{1}{p_m}V\left(x(t),\theta(t)\right)}\right) \leq \gamma_1^{-1}\left(\sqrt{\frac{1}{p_m}V(x(0),\theta(0))e^{-\frac{c}{2}t}}\right) \\
&\leq \gamma_1^{-1}\left(\sqrt{\frac{p_M}{p_m}}\,|z(x(0),\theta(0))|\, e^{-\frac{c}{2}t}\right) \leq \gamma_1^{-1}\left(\sqrt{\frac{p_M}{p_m}}\gamma_2\left(|x(0) - \xi(\theta(0))|\right) e^{-\frac{c}{2}t}\right) \\
&\leq \gamma_1^{-1}\left(\sqrt{\frac{p_M}{p_m}}\gamma_2\left(|x(0)|_\Xi + d\right) e^{-\frac{c}{2}t}\right) = \beta\left(\left[|x(0)|_\Xi + d\right], \ t\right), \qquad \forall t \geq 0
\end{aligned} \tag{3.32}$$

which explicitly states uniform global attractivity of $\Xi \times J_\theta$.

To satisfy (2.26), let $\omega_s = \mu V^\theta(x,\theta)$ in (2.25). This results in the closed-loop

$$\begin{aligned} \dot{x} &= \tilde{f}(x,\theta) + \tilde{g}(x,\theta)\, \upsilon_s(\theta) \\ \dot{\theta} &= \upsilon_s(\theta) - \mu V^\theta(x,\theta) \end{aligned} \tag{3.33}$$

which has the same form as (1.10). Some issues regarding the minimization of $V(x,\theta)$ with respect to θ need to be resolved. As shown in the motivational example, $V(x,\cdot)$ may have multiple minima which means that the initial search point $\theta(0)$ must be restricted to a local set. There may also be points x in $\mathbb{R}^{nm}$ where this minimization is not feasible. For instance, in the example with the circular path, if $x=0$ (and $P=I$), then the entire circle is an extremum. We make the assumption:

Assumption 3.1. *There exist $\rho > 0$ such that for every fixed x with $|x|_\Xi \le \rho$ implies that $V(x,\cdot)$ has a global minimizer, denoted $\theta_V(x)$, which is a LAS equilibrium for*

$$\dot{\theta} = -V^\theta(x,\theta) \tag{3.34}$$

and with basin of attraction $\mathcal{H}_g(x)$. The function $x \mapsto \theta_V(x)$ is locally Lipschitz on $\{x : \ |x|_\Xi \le \rho\}$.

Define the set

$$\mathcal{H}(\rho) := \{(x,\theta) : \ |x|_\Xi \le \rho, \ \theta \in \mathcal{H}_g(x)\}. \tag{3.35}$$

Choosing μ sufficiently large in (3.33) induces a separation of time scales between the plant dynamics $x(t)$ and the set parameter $\theta(t)$. Letting $\varepsilon = \frac{1}{\mu}$ be small, allows for (3.33) to be analyzed as a singularly perturbed system (see [8, 9, 5]). Let $t_f = \frac{1}{\varepsilon}t$ and define $x' := \frac{dx}{dt_f}$. In the fast time scale t_f, the rapid transient of θ is approximately described by the boundary layer system at $\varepsilon = 0$:

$$x' = 0, \qquad \theta' = -V^\theta(x,\theta).$$

By construction, the set $\{(x,\theta) : \ \theta = \theta_V(x)\}$ is AS for $(x(0),\theta(0)) \in \mathcal{H}(\rho)$ as defined in (3.35). The fast variable θ therefore rapidly converges to a slow manifold $\mathcal{M}_\varepsilon$ located in the ε-neighborhood of the manifold $\mathcal{M}_\theta$ defined by $V^\theta(x,\theta) = 0$. With θ constrained to be the solution to the minimization problem, $\theta = \theta_V(x)$, we get the reduced system

$$\dot{x} = \tilde{f}(x,\theta_V(x)) + \tilde{g}(x,\theta_V(x))\, \upsilon_s(\theta_V(x)) \tag{3.36}$$

for which we consider the energy function $W(x) := V(x,\theta_V(x)) = |x|^2_{\Xi,V}$. Using the identities

$$\begin{aligned} V^x(x,\theta)\tilde{f}(x,\theta) &= -z(x,\theta)^\top Q z(x,\theta) \\ V^x(x,\theta)\tilde{g}(x,\theta) &= -V^\theta(x,\theta) \\ V^\theta(x,\theta_V(x)) &= 0 \end{aligned}$$

then for $|x(0)|_\Xi \le \frac{p_m}{p_M}\rho$, we have

$$\dot{W}(x) = -z(x,\theta_V(x))^\top Q z(x,\theta_V(x)) \le -cW(x) \tag{3.37}$$

and the following relationships hold

$$
\begin{aligned}
|x(t)|_{\Xi} &\leq |x(t)-\xi(\theta_z(x(t)))| \leq \gamma_1^{-1}\left(|x(t)|_{\Xi,z}\right) \leq \gamma_1^{-1}\left(|z\left(x(t),\theta_V(x(t))\right)|\right) \\
&\leq \gamma_1\left(\sqrt{\frac{1}{p_m}}\,|x(t)|_{\Xi,V}\right) \leq \gamma_1^{-1}\left(\sqrt{\frac{1}{p_m}W\left(x(0)\right)}e^{-\frac{\varepsilon}{2}t}\right) \leq \gamma_1^{-1}\left(\sqrt{\frac{1}{p_m}V\left(x(0),\bar{\theta}(x(0))\right)}e^{-\frac{\varepsilon}{2}t}\right) \\
&\leq \gamma_1^{-1}\left(\sqrt{\frac{p_M}{p_m}}\left|z\left(x(0),\bar{\theta}(x(0))\right)\right|e^{-\frac{\varepsilon}{2}t}\right) \leq \gamma_1^{-1}\left(\sqrt{\frac{p_M}{p_m}}\gamma_2\left(\left|x(0)-\xi(\bar{\theta}(x(0)))\right|\right)e^{-\frac{\varepsilon}{2}t}\right) \\
&= \gamma_1^{-1}\left(\sqrt{\frac{p_M}{p_m}}\gamma_2\left(|x(0)|_{\Xi}\right)e^{-\frac{\varepsilon}{2}t}\right) = \beta\left(|x(0)|_{\Xi}\,,\ t\right)
\end{aligned} \tag{3.38}
$$

which implies that Ξ is asymptotically stable for the **reduced system.** It follows, according to the main results in [5], that for each $\delta > 0$ there exists a μ large enough so that with proper initial conditions $(x(0), \theta(0))$, the behavior, characterized by the distance to Ξ, of the solutions to (3.33) are δ-close to the corresponding behavior of the reduced system (3.36) for which $\theta(t) = \theta_V(x(t))$, that is

$$|x(t)|_{\Xi} \leq \beta\left(|x(0)|_{\Xi}\,,\ t\right) + \delta, \qquad \forall t \geq 0. \tag{3.39}$$

This bound establishes the *"near forward invariance"* property aimed for. It states, in particular, that for $x(0) \in \Xi$ and θ in a compact subset of $\mathcal{H}_g(x(0))$, the excursion of $x(\cdot)$ from Ξ can be made arbitrarily small. Therefore, (3.32) together with (3.39) yields *"near stability"* of Ξ.

We summarize our result in the following theorem:

Theorem 3.1. *There exist a class-$\mathcal{KL}$ function β and a constant $d = d(x(0), \theta(0)) > 0$ such that, for all initial conditions $(x(0), \theta(0)) \in \mathbb{R}^{nm} \times J_\theta$ and all $\mu > 0$, the trajectories of (3.33) satisfy*

$$|x(t)|_{\Xi} \leq \beta\left(\left[|x(0)|_{\Xi} + d\right],\ t\right), \qquad \forall t \geq 0 \tag{3.40}$$

and, under Assumption 3.1, for each $\delta > 0$ and each compact set $\mathcal{K} \subseteq \mathcal{H}\left(\frac{p_m}{p_M}\rho\right)$ there exists $\mu^* > 0$ such that $\mu \geq \mu^*$ and $(x(0), \theta(0)) \in \mathcal{K}$ imply

$$|x(t)|_{\Xi} \leq \beta\left(|x(0)|_{\Xi}\,,\ t\right) + \delta, \qquad \forall t \geq 0. \tag{3.41}$$

3.2 Remark: The 2^{nd} order gradient algorithm

In [4], the CLF (2.24) was extended with the term $\frac{\varepsilon}{2\mu}\omega_s^2$ to construct an $\dot{\omega}_s$ -update law. Differentiating the extended CLF, the 2^{nd} order controller dynamics was designed as

$$\dot{\theta} \;=\; \upsilon_s(\theta) - \omega_s \tag{3.42}$$

$$\varepsilon\dot{\omega}_s \;=\; -\omega_s + \mu V^{\theta}(x,\theta). \tag{3.43}$$

By setting $\varepsilon = 0$, we can again apply singular perturbation techniques on the closed-loop system where x and θ are the slow states and ω_s are the fast state which rapidly converges to an ε-neighborhood of the manifold $\omega_s - \mu V^{\theta}(x,\theta) = 0$. Substituting the constraint $\omega_s = \mu V^{\theta}(x,\theta)$ into (3.42) gives the reduced system

$$
\begin{aligned}
\dot{x} &= \tilde{f}(x,\theta) + \tilde{g}(x,\theta)\upsilon_s(\theta) \\
\dot{\theta} &= \upsilon_s(\theta) - \mu V^{\theta}(x,\theta)
\end{aligned} \tag{3.44}
$$

which approximately describes the motion of x and θ in the slow time-scale. This reduced system is exactly the closed-loop (3.33). Consequently, if ε is chosen small and μ large, then the results of near forward invariance from the previous analysis are recovered 'approximately'.

4 Case: Maneuvering a ship into a harbour

We consider the high-speed container ship of length $L = 175\,\mathrm{m}$ used in [4]. Let $\eta = [x\ y\ \psi]^\top$ be the Earth-fixed position vector, where (x, y) is the position of the body frame on the ocean surface, and ψ is the yaw angle. Let $\nu = [u\ v\ r]^\top$ be the velocity vector of the body frame, where u and v are the surge and sway speeds, and r is the yaw rate. The kinematic and dynamic equations are then the 3 degree of freedom (DOF) model

$$\begin{aligned} \dot{\eta} &= J(\psi)\nu \\ M\dot{\nu} + n(\nu) &= B(\nu)\,\tau \end{aligned} \tag{4.45}$$

where $J(\psi) \in SO(3)$ is the 3×3 rotation matrix, M is the system inertia matrix, and $n(\nu)$ is a vector incorporating coriolis and hydrodynamic damping.

The available control τ and the actuator configuration matrix $B(\nu)$ is dependent on the speed and operation to be performed. In a high-speed cruise operation, the ship is only actuated by an aft propeller and a rudder so that $\tau = \tau_c = [T_u,\ \delta_R]^\top$ and $B = B_c \in \mathbb{R}^{3\times 2}$. In a low-speed docking operation, an additional bow thruster can be activated, yielding $\tau = \tau_d = [T_u,\ \delta_R,\ T_b]^\top$ and $B = B_d \in \mathbb{R}^{3\times 3}$.

In this illustration, we investigate the scenario of a ship arriving at a harbour. As the ship enters, it has to change from a high-speed cruise operation to a low-speed docking operation, and adjustments to the path definition, the speed assignment, and the controller algorithms are necessary. Figure 4 depicts the situation where $\{E_1\}$ is the earth-fixed inertial frame, and $\{E_2\}$ is

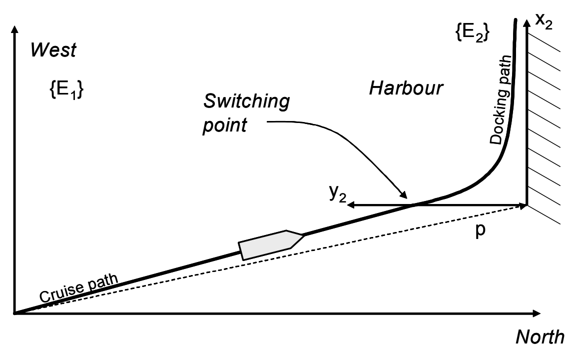

Figure 4: Sketch of the control scenario; a ship following a cruise path must switch to a docking operation when it enters the harbour.

a local "harbour" frame located at p and rotated by a fixed angle β, here 90°, in $\{E_1\}$.

Next, one maneuvering controller is developed for each operation using the procedure in [4]. For the cruise operation, we will control a 3DOF model with only 2 controls. When controlling only the position (x, y) in (4.45), it was shown originally in the master thesis of K. P. Lindegaard (1997) and later in [10, 11] how the uncontrolled yaw dynamics are stabilized if the output map $h(\eta)$ of the ship are chosen as coordinates in the bow (or even ahead) of the ship. Motivated by these results, we choose output coordinates l_x meters ahead on the x-axis of the body frame. Let $l := [l_x\ 0]^\top$ and define the matrices

$$\Pi_1 := \begin{bmatrix} 1 & 0 & 0 \\ 0 & 1 & 0 \end{bmatrix} \quad \Pi_2 := \begin{bmatrix} 1 & 0 & 0 \\ 0 & 1 & l_x \end{bmatrix} \quad \Pi_3 := \begin{bmatrix} \Pi_2 \\ [0\,0\,1] \end{bmatrix}$$

$$R(\psi) := \begin{bmatrix} \cos\psi & -\sin\psi \\ \sin\psi & \cos\psi \end{bmatrix} \quad J(\psi) = \begin{bmatrix} R(\psi) & 0 \\ 0 & 1 \end{bmatrix} \quad S_2(r) := \begin{bmatrix} 0 & -r \\ r & 0 \end{bmatrix} \quad S_3(r) := \begin{bmatrix} S_2(r) & 0 \\ 0 & 0 \end{bmatrix}$$

Let the subscripts c and d denote cruise and docking operation respectively. Then the output state $x_{1c} := \Pi_1\eta + R(\psi)l$ is the coordinate vector in the bow of the ship where l_x is left free. For docking, we have increased control and add the yaw state, $x_{1d} := [x_{1c}^\top\ \psi]^\top$. The corresponding body-fixed velocity vectors are $x_{2c} := \Pi_1\nu + S(r)l = \Pi_2\nu$ and $x_{2d} := [x_{2c}^\top\ r]^\top$. This gives the reduced 4 state model for cruise operation

$$\begin{aligned} \dot{x}_{1c} &= R(\psi)x_{2c} \\ \dot{x}_{2c} &= \Pi_2 M^{-1}\left[B_c(\nu)\tau - n(\nu)\right] = B_{uc}(\nu)\tau - \Pi_2 M^{-1}n(\nu) \end{aligned} \tag{4.46}$$

and the 6 state docking model

$$\begin{aligned} \dot{x}_{1d} &= J(\psi)x_{2d} \\ \dot{x}_{2d} &= \Pi_3 M^{-1}\left[B_d(\nu)\tau - n(\nu)\right] = B_{ud}(\nu)\tau - \Pi_3 M^{-1}n(\nu) \end{aligned} \tag{4.47}$$

where $B_{uc} \in \mathbb{R}^{2\times 2}$ and $B_{ud} \in \mathbb{R}^{3\times 3}$ are invertible for all ν. Let the desired paths for x_{1c} and x_{1d} be $\xi_c(\theta) = [x_r(\theta),\ y_r(\theta)]^\top$ and $\xi_d(\theta) = \left[x_r(\theta),\ y_r(\theta),\ \arctan\left(\frac{y_r^\theta(\theta)}{x_r^\theta(\theta)}\right)\right]^\top$, and the speed assignments are $\upsilon_c(\theta, t)$ and $\upsilon_d(\theta, t)$. Application of the procedure in [4] on (4.46) and (4.47) gives

<u>*Cruise Operation* :</u>	<u>*Docking Operation* :</u>
$z_{1c} = x_{1c} - \xi_c(\theta)$	$z_{1d} = x_{1d} - \xi_d(\theta)$
$z_{2c} = x_{2c} - \alpha_{1c}(x_{1c}, \theta, t)$	$z_{2d} = x_{2d} - \alpha_{1d}(x_{1d}, \theta, t)$
$\alpha_{1c} = R^\top(\psi)\left[A_{1c}z_{1c} + \xi_c^\theta(\theta)\upsilon_c(\theta, t)\right]$	$\alpha_{1d} = J^\top(\psi)\left[A_{1d}z_{1d} + \xi_d^\theta(\theta)\upsilon_d(\theta, t)\right]$
$\sigma_{1c} = R^\top(\psi)\left[A_{1c}R(\psi)x_{2c} + \xi_c^\theta(\theta)\upsilon_c^t(\theta, t)\right]$	$\sigma_{1d} = J^\top(\psi)\left[A_{1d}J(\psi)x_{2d} + \xi_d^\theta(\theta)\upsilon_d^t(\theta, t)\right]$
$\quad -S_2(r)\alpha_{1c}$	$\quad -S_3(r)\alpha_{1d}$
$\nu_{2c} = R^\top(\psi)[-A_{1c}\xi_c^\theta(\theta)$	$\nu_{2d} = J^\top(\psi)[-A_{1d}\xi_d^\theta(\theta)$
$\quad +\xi_c^{\theta^2}(\theta)\upsilon_c(\theta, t) + \xi_c^\theta(\theta)\upsilon_c^\theta(\theta, t)]$	$\quad +\xi_d^{\theta^2}(\theta)\upsilon_d(\theta, t) + \xi_d^\theta(\theta)\upsilon_d^\theta(\theta, t)]$
$\Downarrow$ *Control* :	$\Downarrow$ *Control* :
$\tau_c = B_{uc}^{-1}(\nu)[-P_{2c}^{-1}R^\top P_{1c}z_{1c} + A_{2c}z_{2c}$	$\tau_d = B_{ud}^{-1}(\nu)[-P_{2d}^{-1}J^\top P_{1d}z_{1d} + A_{2d}z_{2d}$
$\quad +\Pi_2 M^{-1}n(\nu) + \sigma_{1c} + \nu_{2c}\upsilon_c]$	$\quad +\Pi_3 M^{-1}n(\nu) + \sigma_{1d} + \nu_{2d}\upsilon_d]$
$\Downarrow$ *2nd order update law* :	$\Downarrow$ *2nd order update law* :
$\dot{\theta} = \upsilon_c(\theta) - \omega_s$	$\dot{\theta} = \upsilon_d(\theta) - \omega_s$
$\dot{\omega}_s = -\lambda\omega_s - 2\mu\lambda\left[z_{1c}^\top P_{1c}\xi_c^\theta(\theta) + z_{2c}^\top P_{2c}\nu_{2c}\right]$	$\dot{\omega}_s = -\lambda\omega_s - 2\mu\lambda\left[z_{1d}^\top P_{1d}\xi_d^\theta(\theta) + z_{2d}^\top P_{2d}\nu_{2d}\right]$

where $A_{1(\cdot)}$ and $A_{2(\cdot)}$ are Hurwitz design matrices for which $P_{1(\cdot)}$ and $P_{2(\cdot)}$ satisfy the respective Lyapunov equations. Since the yaw dynamics (ψ, r) are not directly controlled in cruise operation, a full control synthesis should include an analysis of the zero dynamics. However, this is not conceptually important in this example, and we refer the reader to results in [10, 11] on these issues.

According to Figure 4, the cruise path is simply parametrized by θ as a straight line in the frame of $\{E_1\}$, and the docking path is an exponentially decaying curve in $\{E_2\}$, that is

$$\text{Cruise path:} \quad \begin{bmatrix} x_r(\theta) \\ y_r(\theta) \end{bmatrix} = \begin{bmatrix} \theta \\ k_c\theta \end{bmatrix} \qquad \text{Docking path:} \quad \begin{bmatrix} x_r(\theta) \\ y_r(\theta) \end{bmatrix} = \begin{bmatrix} \theta \\ k_d e^{-\frac{1}{T_d}\theta} + k_0 \end{bmatrix} \tag{4.48}$$

where k_0 denotes the offset from the quay and is thus determined by the breadth of the ship.

If $u_d = u_d(\theta, t)$ is the desired surge speed along the path, then the general speed assignment is

$$\begin{aligned} \upsilon_s(\theta,t) &= \frac{u_d(\theta,t)}{\sqrt{x_r^\theta(\theta)^2 + y_r^\theta(\theta)^2}} \\ \upsilon_s^t(\theta,t) &= \frac{u_d^t(\theta,t)}{\sqrt{x_r^\theta(\theta)^2 + y_r^\theta(\theta)^2}} \\ \upsilon_s^\theta(\theta,t) &= \frac{\left[x_r^\theta(\theta)^2 + y_r^\theta(\theta)^2\right] - \left[x_r^\theta(\theta)x_r^{\theta^2}(\theta) + y_r^\theta(\theta)y_r^{\theta^2}(\theta)\right]}{\left[x_r^\theta(\theta)^2 + y_r^\theta(\theta)^2\right]^{3/2}} u_d^\theta(\theta,t). \end{aligned}$$

In cruise operation, we want the surge speed u_d to be adjustable online by constant set-points u_0 specified by the pilot. Hence, $u_d(\theta,t) = u_0$ and $u_d^\theta = u_d^t = 0$. In the docking operation, the surge speed will be ramped down to zero, that is

$$u_d(\theta) = u_0\left(1 - \frac{1}{\theta_{stop}}\theta\right), \qquad u_d^\theta = -\frac{1}{\theta_{stop}}u_0, \quad u_d^t = 0.$$

To finalize the design, simple logic is used to switch algorithms and to reinitialize $\theta(t)$ from θ_{switch} to 0 when the operation change.

This combined control problem of cruising and docking can be viewed as two separate set stabilization problems. The target sets according to (3.30) and (2.23) are

$$\begin{aligned} \Xi_c &= \left\{ x_c \in \mathbb{R}^4 : \begin{array}{l} x_{1c} = \xi_c(\phi) \\ x_{2c} = \alpha_{1c}(\xi_c(\phi), \phi) = R^\top(\psi_r)\xi_c^\theta \upsilon_c \end{array}, \quad \phi \in \mathbb{R} \right\} \\ \Xi_d &= \left\{ x_d \in \mathbb{R}^6 : \begin{array}{l} x_{1d} = \xi_d(\phi) \\ x_{2d} = \alpha_{1d}(\xi_d(\phi), \phi) = J^\top(\psi_r(\phi))\xi_d^\theta(\phi)\upsilon_d(\phi) \end{array}, \quad \phi \in \mathbb{R} \right\}. \end{aligned}$$

Clearly, discontinuities occur at the point of switching operation and when the pilot changes speed set-points for u_0.

In the simulation, the numerical values for the ship are hydrodynamic coefficients found in [12, Appendix E.1.3]. The forward thrust T_u saturates at 10^6 N and the rudder at $\pm 20\,°$. The harbour frame is located at $p = [5500,\ 2000]^\top$, and the path parameters are $k_c = 0.4$, $k_d = 470$, $k_0 = 30$ and $T_d = 188$. For the speed assignment, an initial surge speed of $u_0 = 14$ knots was specified, and then, before entering the harbour, at time $t = 550$ s, the speed is reduced to $u_0 = 5$ knots. In the docking operation, this speed is ramped down with stop at $\theta_{stop} = 1250$ m. The output coordinates were set by $l_x = 100$ m.

To illustrate the near forward invariance property, the ship equations (4.46) are initialized in the set Ξ_c, that is $(x_{1c}(0), x_{2c}(0)) \in \Xi_c$ at $\phi = 0$, while $\theta(0) = 5000$ and $\omega_s(0) = 0$. This means that $\theta(t)$

must rapidly traverse 5000 m before converging to the global minimizer $\bar{\theta}(x_c(0)) = \theta_{V_c}(x_c(0)) = 0$. In the simulation, the cruise and docking paths were accurately traced, and the transients at the passage through the switching points were insignificant. The surge speed response are plotted in Figure 5a) and is seen to comply with the commanded speeds well. In Figure 5b), the initial error transients of $|x_c(t)|_{\Xi_c,V_c}$ due to the convergence of $\theta(t)$ to the minimizer are plotted for increasing gains λ and μ. Clearly, the transient error decreases as the speed of convergence of $\theta(t)$ increases by higher gains.

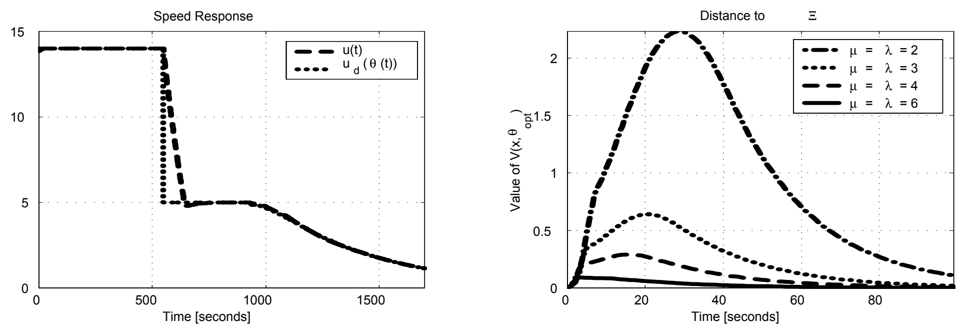

Figure 5: **a)** Surge speed response of the ship. **b)** Initial transients in $|x_c(t)|_{\Xi_c,V_c}$ for increasing gains λ and μ.

5 Conclusion

This paper has studied the problem of stabilizing sets parametrized by a single variable. In the introductory example of stabilizing the unit circle, a dynamic control was developed that rendered the circle uniformly globally attractive. Forward invariance of the circle, on the other hand, was not achieved, and as a result did the control law fail to render the circle UGES. Nevertheless, the control law was equipped with an inherent dynamic gradient minimization algorithm, and with the exact solution to this minimization problem substituted into the closed-loop, the circle was indeed exponentially stable. It was then shown that any level of accuracy of the approximation to the exact solution could be achieved by adjusting the gain μ of the gradient algorithm high enough, and this concept was termed *near forward invariance* of the set.

Recently, in [3, 4] the Maneuvering Problem was introduced and a procedure for solving it for plants in strict feedback form (2.19) was proposed. Characterizing the desired path (and the speed assignment) in the state space as a target set Ξ, it was shown that the maneuvering problem fall into the same category of set stabilization problems as the unit circle example. Indeed, the dynamic update law proposed in [4] are a dynamic gradient minimization algorithm, and, hence, the same analysis can be applied for those systems. As a result, the properties of uniform global attractivity and near forward invariance of the target set Ξ hold for maneuvering systems with the implication this has with respect to stability and performance.

In the final case, the objective of maneuvering a ship into a harbour was illustrated. With the properties of set stabilization discussed in the earlier section, the desired level of performance was achieved for the simulation.

Acknowledgement: Thanks to Thor I. Fossen for valuable discussions on the ship maneuvering case. Research supported by the Norwegian Research Council through the Strategic University Program on Marine Control, and also in part by the NSF under grant ECS-9988813 and by the AFOSR under grant F49620-00-1-0106.

References

[1] J. Hauser and R. Hindman, "Maneuver regulation from trajectory tracking: Feedback linearizable systems," in *Proc. IFAC Symposium on Nonlinear Control Systems Design*, (Lake Tahoe, CA, USA), pp. 595–600, IFAC, June 1995.

[2] R. Hindman and J. Hauser, "Maneuvering modified trajectory tracking," in *Int. Symp. Mathematical Theory Networks and Systems*, (St. Louis, MO, USA), June 1996.

[3] R. Skjetne, T. Fossen, and P. Kokotović, "Output maneuvering for a class of nonlinear systems," in *Proc. 15th IFAC World Congress Automatic Control*, (Barcelona, Spain), July 2002.

[4] R. Skjetne, T. Fossen, and P. Kokotović, "Robust output maneuvering for a class of nonlinear systems," *Automatica*. Submitted May 7th, 2002.

[5] A. R. Teel, L. Moreau, and D. Nešić, "A unified framework for input-to-state stability in systems with two time scales," *IEEE Trans. Automat. Contr.*, 2002. Submitted June 12, 2001.

[6] A. Teel and L. Praly, "A smooth lyapunov function from a class-$\mathcal{KL}$ estimate involving two positive semidefinite functions," *ESAIM: Control, Optimisation and Calculus of Variations*, vol. 5, pp. 313–367, 2000.

[7] A. Filippov, *Differential Equations with Discontinuous Right-hand sides.* Kluwer Academic Publishers, 1988.

[8] P. Kokotović, H. K. Khalil, and J. O'Reilly, *Singular perturbation methods in control.* Philadelphia, PA: Society for Industrial and Applied Mathematics (SIAM), 1999. Analysis and design, Corrected reprint of the 1986 original.

[9] H. K. Khalil, *Nonlinear Systems.* New Jersey: Prentice-Hall, Inc., 3 ed., 2002.

[10] T. Fossen, J. Godhavn, S. Berge, and K. Lindegaard, "Nonlinear control of underactuated ships with forward speed compensation," in *Proc. 4th IFAC Nonlinear Control Systems Design Symposium*, (Enschede, the Netherlands), pp. 121–126, IFAC, July, 1-3 1998.

[11] S. Berge, K. Ohtsu, and T. Fossen, "Nonlinear control of ships minimizing the position tracking errors," in *Proc. IFAC Conf. Contr. Appl. Marine Systems (CAMS)*, (Fukuoka, Japan), pp. 141–146, IFAC, Oct, 27-30 1998.

[12] T. Fossen, *Guidance and Control of Ocean Vehicles.* England: John Wiley & Sons Ltd., 1994.